Bull. Mater. Sci., Vol. 34, No. 5, August 2011, pp. 1033–1037. © Indian Academy of Sciences.

# Synthesis of Mn-doped $CeO_2$ nanorods and their application as humidity sensors

**C H HU, C H XIA*, F WANG, M ZHOU, P F YIN and X Y HAN**
Science College of Chongqing Jiaotong University, Chongqing 400074, PR China

MS received 10 October 2010; revised 21 December 2010

**Abstract.** **Mn-doped $CeO_2$ nanorods have been prepared from $CeO_2$ particles through a facile composite-hydroxide-mediated (CHM) approach. The products were characterized by X-ray diffraction (XRD), scanning electron microscopy (SEM) and transmission electron microscopy (TEM). The analysis from the X-ray photoelectron spectroscopy indicates that the manganese doped in $CeO_2$ exists as $Mn^{4+}$. The responses to humidity for static and dynamic testing proved doping Mn into $CeO_2$ can improve the humidity sensitivity. For the sample with Mn% about 1·22, the resistance changes from 375·3 to 2·7MΩ as the relative humidity (RH) increases from 25 to 90%, indicating promising applications of the Mn-doped $CeO_2$ nanorods in environmental monitoring.**

**Keywords.** **Mn-doped $CeO_2$; nanorods; humidity sensitivity.**

## 1. Introduction

It is well known that rare earth oxides have been widely used in electronics, magnetic, chemical engineering, and functional materials for their special characteristics. Cerium oxides have been found to be highly interesting materials in processes related to the production of hydrogen for fuel cells (Fu *et al* 2006; Kim and Thompson 2006) or the abatement of organic pollutants from industrial wastewater (Blanco *et al* 2004; Goi *et al* 2004). Likewise they are being used as polishing materials in optics (Kosynkin *et al* 2000), as components of oxygen sensors (Stefanik and Tuller 2001) or as efficient catalyst (Leandro *et al* 2009). More recently, ceria doped with metal ion has exhibited novel properties in many aspects. Corma *et al* (2004) prepared organic-dye-free solar cells using ceria nanoparticles. They found that $CeO_2$ nanoparticles as well as rare-earth-doped ceria do not need photosensitization to have photovoltaic activity in the visible region, and the excitation spectrum depended notably on the presence of dopants. $CeO_2$ with fluorite-type structure is known to tolerate a considerable reduction without phase change and is also known to show relatively high oxide ion conductivity. In addition, the reduction of $Ce^{4+}$ results in the simultaneous formation of oxide ion vacancy (Teraoka *et al* 1999), causing the appearance of electronic conductivity and thus being a mixed conductor. The mixed conductivity of ceria-based materials might be enhanced when a transition metal ion, the valence of which is lower than 4+, is incorporated into ceria to form a solid solution; increases in the amount of oxide ion vacancies by the substitution with a lower-valence cation and the electronic conductivity originating from the nature of a transition metal ion might be expected. So many studies have been carried out based on the Mn-doped $CeO_2$ (Kang *et al* 2006; Wu *et al* 2007; Shan *et al* 2010). The materials used for humidity sensors are generally organic polymers or metal oxides. Humidity sensors based on organic polymer have many challenges due to their weak mechanical strength and poor physical and chemical stabilities. Ceramic type of humidity sensors are superior in performance to the polymeric type, because of its high stability towards a variety of chemical species, wide range of operating temperatures and fast response to the changes of humidity. The recent investigations suggest that humidity sensors based on $CeO_2$ powder show poor sensitivity (Parvatikar *et al* 2006), but the humidity sensor based on $CeO_2$ doped with Ba has shown a fast response (Zhang Z W *et al* 2007).

In this paper, to explore properties of the metal-doped $CeO_2$ nanorods, we synthesized Mn-doped $CeO_2$ nanorods by the composite-hydroxide-mediated (CHM) approach, which is based on chemical reactions of materials in eutectic hydroxide melts at a temperature of 165–200°C and ambient pressure in the absence of organic dispersants or capping reagents (Hu *et al* 2006; Wang *et al* 2007; Zhang Z W *et al* 2007). The as-synthesized nanorods were characterized by X-ray diffraction (XRD), scanning electron microscopy (SEM), transmission electron microscopy (TEM) and X-ray photoelectron spectroscopy (XPS). The humidity sensitivity of Mn-doped $CeO_2$ nanorods was investigated.

*Author for correspondence (xxhkaixin@163.com)

## 2. Experimental

### 2.1 *Material preparation*

Mn-doped $CeO_2$ nanorods were synthesized by CHM method. In a typical synthesis process, an amount of 9 g mixed NaOH and KOH with a ratio of 51·5:48·5 was placed in a 25 mL Teflon vessel. A mixture of 1 mmol $CeO_2$ and 1 mmol $MnCl_2$ were added into the vessel as reactants for reaction. Then, the vessel was put into a furnace preheated to 200°C. After reacting for 24 h (sample 1), 48 h (sample 2) and 72 h (sample 3), respectively the vessels were taken out and cooled to room temperature. The products from the reaction were washed by deionized water for several times.

### 2.2 *Characterization*

The X-ray diffractometer (XRD), energy dispersive X-ray spectroscopy (EDS) and X-ray photoelectron spectrum (XPS) were used to investigate the crystalline phase and chemical composition of the samples. The field emission scanning electron microscopy (SEM) and transmission electron microscopy (TEM) were used to characterize the morphology and size of the as-synthesized samples.

### 2.3 *Humidity sensitivity*

Thin films for humidity sensitivity sensors were prepared by source $CeO_2$ particles and Mn-doped $CeO_2$ nanorods. The samples were first dispersed in ethanol, and then dropped on top of pre-deposited Au electrodes on the surface of Si wafer. The dimension of the film was 5 mm in length, 3 mm in width, and ∼20 μm in thickness. Ohmic contact for the planar film with copper wires was made by silver paste. The measurements were carried out by putting the sensors in an airproof glass vessel with a volume of 2 L. A hygroscope was placed into the vessel to monitor the relative humidity during the experiment. The sensor's resistance is measured by an external testing circuit.

## 3. Results and discussion

### 3.1 *Crystal phase*

Figure 1 shows XRD spectra of the as-synthesized Mn-doped $CeO_2$ growing at 200°C for 72 h. All peaks of the three samples can be indexed as the cubic phase (*Fm*3*m*, JCPDS 34–0394) with lattice constant $a = 0{\cdot}5411$ nm which belongs to the $CeO_2$ and have no other peaks. So we think that the Mn ions have entered into the lattice of $CeO_2$. We also find that diffraction peaks of the Mn-doped $CeO_2$ slightly shift to larger Bragg angles, indicating that part of manganese species might have entered into the lattice (Machida *et al* 2000). One possible explanation might be that the

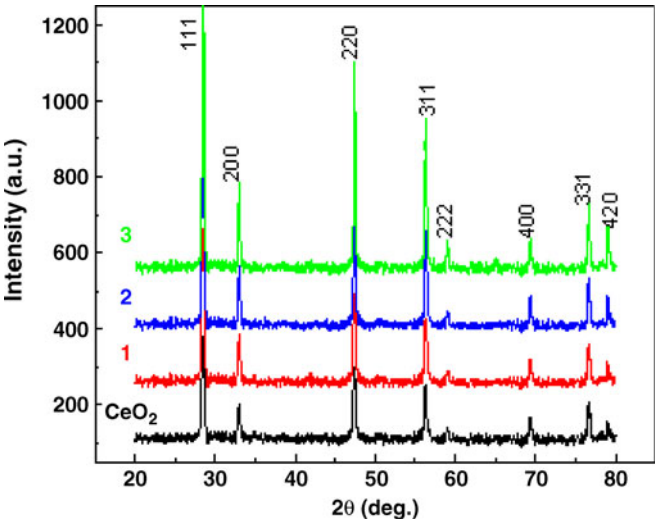


**Figure 1.** XRD spectra of source material $CeO_2$ and as synthesized Mn-doped $CeO_2$ grown at 200°C for 24 h (sample 1), 48 h (sample 2) and 72 h (sample 3).

incorporation of the lattice parameters as the ionic radius of $Mn^{4+}$ (0·056 nm) and $Mn^{3+}$ (0·062 nm) are smaller than that of $Ce^{4+}$ (0·097 nm) (Wu *et al* 2007).

### 3.2 *Morphology and microstructure characterization*

Figure 2 shows SEM images of the source material $CeO_2$ (a) and Mn-doped $CeO_2$ sample (b). The particle morphology of the source material, $CeO_2$ with a diameter ranging from 500 nm–1 μm can be seen. When doped with Mn, the particles convert gradually into nanorods with a length of 2–4 μm. The morphology of the three Mn-doped $CeO_2$ are nearly the same, so we only put one picture here. The EDS in the inset of figure 2b indicates the existence of Ce, Mn and O in the nanorods. Here, the C signal comes from the substrate. Figures 2c-d and the inset in d are the TEM images and SAED patterns of Mn-doped $CeO_2$ nanorods. The SAED pattern of the corresponding edge of the nanorod in figure 2d demonstrates the single crystalline structure.

The constituents and valence states at the surface were investigated by XPS. All binding energies have been corrected for the charging effect with reference to the C 1*s* line at 284·6 eV. The survey spectrum of the sample (figure 3a) shows peaks corresponding to Ce, Mn and O, ruling out incorporation of any additional impurities during the sample preparation. The XPS spectra of Ce 3*d*, O 1s and Mn 2*p* for three samples are shown in figures 3b, c, d, e, f, respectively. The Ce 3*d* spectrum can be resolved into eight components (Burroughs *et al* 1976). The peaks are assigned for $Ce^{4+}$ as $V$, $V''$ and $V'''$ for Ce $3d_{5/2}$, with the corresponding Ce $3d_{3/2}$ peaks labeled as $U$, $U''$ and $U'''$. And the signals of $Ce^{3+}$ ($V'$ and $U'$) are not observed. The XPS peak positions of Ce 3*d* are listed in table 1. So, the valence state of Ce element does not change after doping with Mn. The XPS spectrum

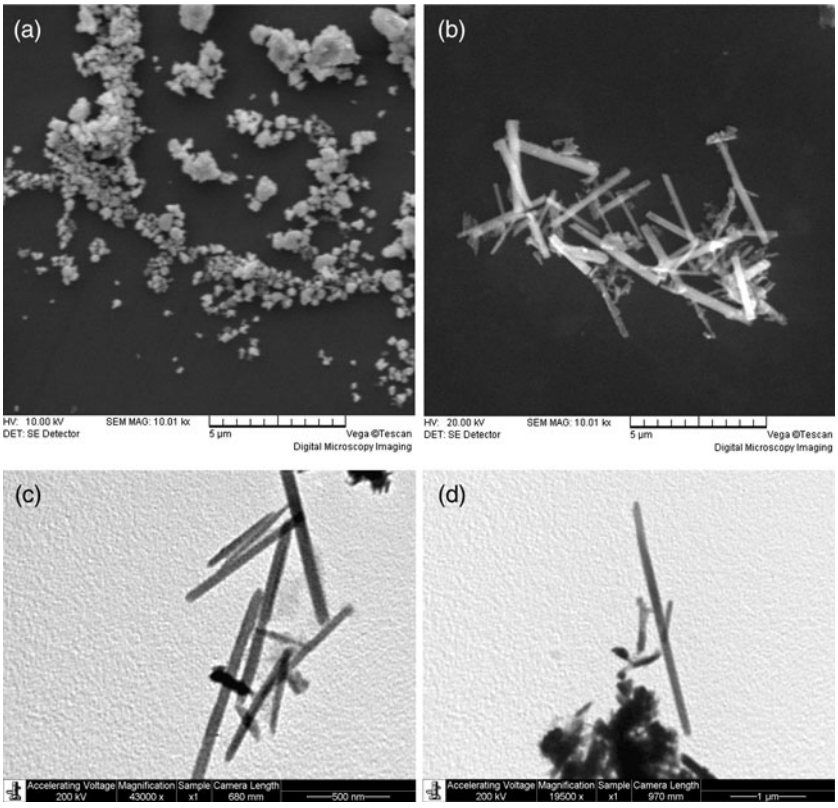


**Figure 2.** SEM images of source material $CeO_2$ (**a**), Mn-doped $CeO_2$ (**b**), EDS (inset of **b**), TEM images (**c**, **d**) and electron diffraction pattern (inset of **d**) of Mn-doped $CeO_2$ sample.

of Mn $2p$ is shown in figure 3c. Both the Mn $2p_{3/2}$ (642·49, 642·48, 642·5 eV) and Mn $2p_{1/2}$ (653·90, 653·89, 653·9 eV) are observed, demonstrating the existence of $Mn^{4+}$ (Wu *et al* 2007) for the three samples. To know the oxygen species on the surface, the O 1*s* spectrum is shown in figure 3d. The O 1*s* peak centred at 529·7 eV corresponds to the contribution of $O^{2-}$ (Zhang D S *et al* 2007). The atomic percentage of Mn in samples 1, 2 and 3 are 0·50, 0·98 and 1·22 at%, respectively.

### 3.3 *Humidity sensitivity*

The humidity sensitivity experiments were performed with humidity sensor devices made from the source material $CeO_2$ and Mn-doped $CeO_2$ samples, as shown in figure 4(a), while the experimental set up is shown in figure 4(b). The humidity in the vessel is controlled by mixing dry air and wet air. The resistances ($R_{RH}$) of the devices vs relative humidity (RH) are shown in figure 5(a), where $R_{RH}$ denotes the resistance of the sensors in different humidity environments. Figure 5(a) represents the $R_{RH}$ response to RH for the devices of the source $CeO_2$ and the Mn-doped $CeO_2$ (1, 2, 3). With increase in humidity, the resistance of the device made of the source material $CeO_2$ changes little, while the resistance of devices made of Mn-doped $CeO_2$ nanorods decreased very fast. For sample 3, the resistance of the device in 25% RH is 375·5MΩ, while it is 7·9MΩ in 90% RH. From this figure, we can see that with more Mn ions incorporated into the $CeO_2$, the resistance decreased more rapidly with increased humidity. The humidity sensitivity $S$ is defined as

$$S = 100\,|R_H - R_O|\,/R_O,$$

where $R_O$ is the initial resistance of the sample and $R_H$ the resistance in 90% RH. The sensitivity of the three samples are 70·79, 80·68 and 97·89, respectively. And the graph is shown in the inset of figure 5(a).

We choose sample 3 to do the dynamic testing. The dynamic testing of the Mn-doped $CeO_2$ device in a certain RH shown in figure 5b provided some important parameters for a sensor device: responses time, recovery time, and reproducibility. We call dry air as DA and wet air as WA in short. The device was put in the vessel with an initial RH of 50% and an initial resistance of about 275 MΩ. When the wet air of about 90% was switched into the vessel, the resistance of the device decreased rapidly. After 1 min, the resistance of the device was reduced to 3 MΩ and then changed slowly. Then the dry air of about 25% RH was switched into the vessel and the resistance recovered to about 275 MΩ in 3 min. Another three circles was followed after the previous one in which the response time was 2 min and

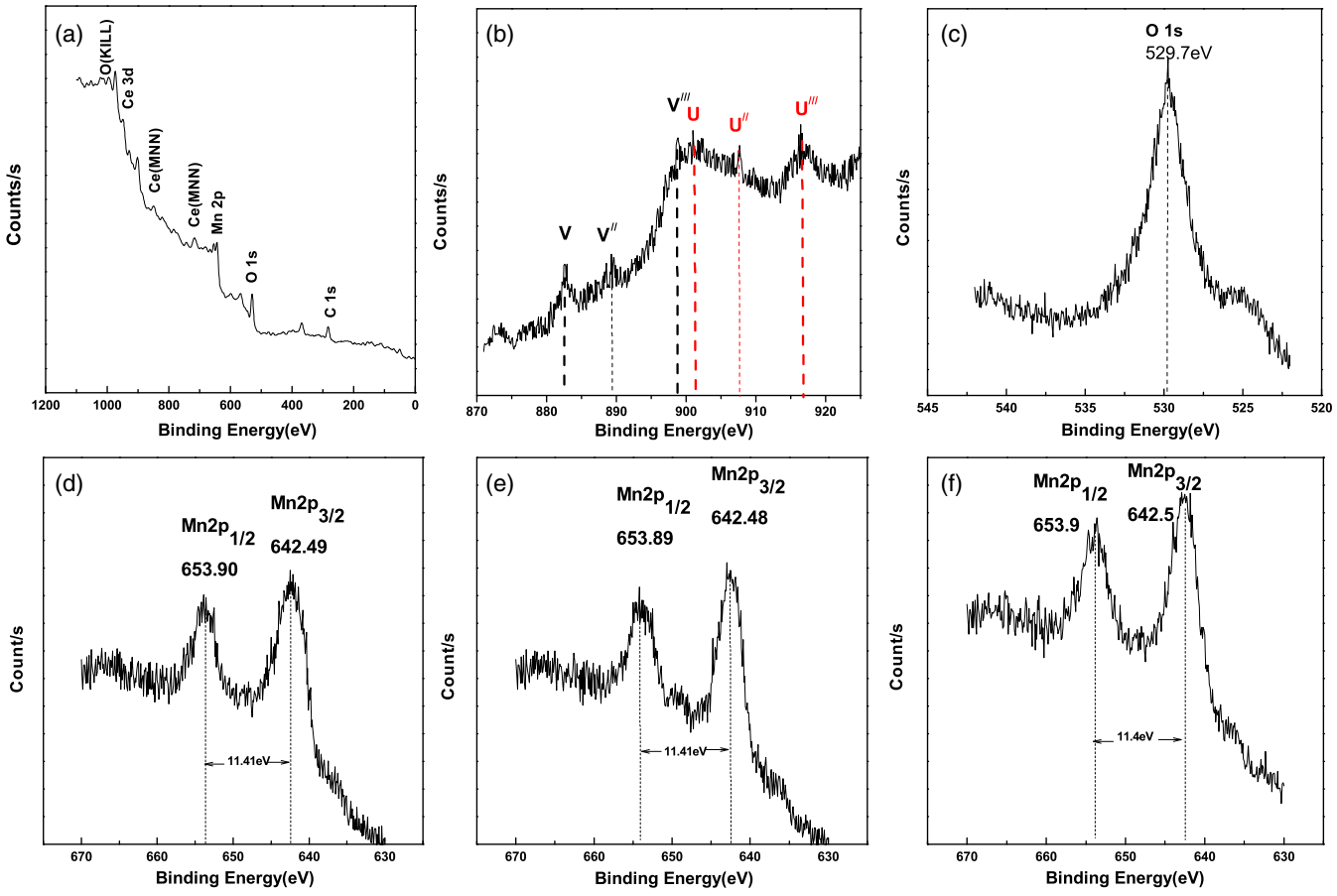


**Figure 3.** XPS integral spectrum (**a**), Ce 3*d* (**b**), O 1*s* (**c**) and Mn 2*p* (**d**, **e**, **f**) and spectrum of Mn-doped $CeO_2$ nanorods.

**Table 1.** XPS peak positions (binding energy, eV) obtained for Mn-doped $CeO_2$ samples (literature values have been added for comparison).

| XPS peaks | Mn-doped $CeO_2$ | $CeO_2$[20] |
|---|---|---|
| Ce $3d_{5/2}$ | | |
| *V* | 882·45 | 882·44–882·58 |
| *V′* | – | 884·59–885·53 |
| *V″* | 889·27 | 888·97–889·21 |
| *V‴* | 898·72 | 898·35–898·50 |
| Ce $3d_{3/2}$ | | |
| *U* | 900·98 | 900·93–901·02 |
| *U′* | – | 903·33–903·91 |
| *U″* | 907·70 | 907·79–907·93 |
| *U‴* | 916·81 | 916·80–916·84 |

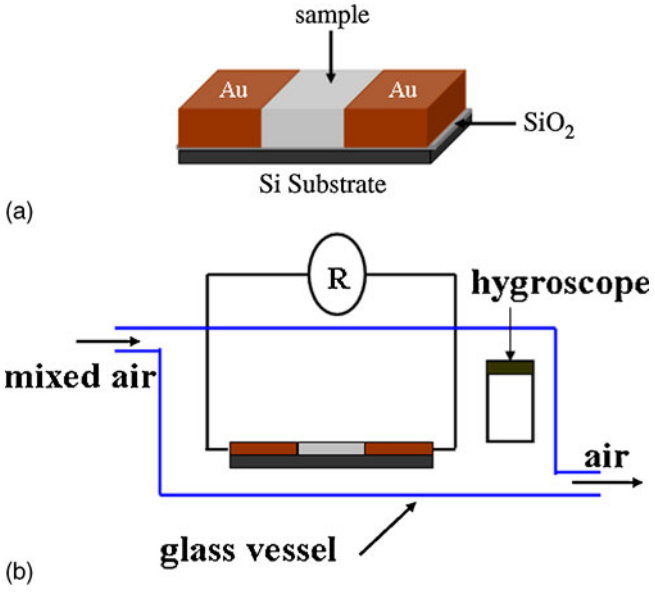


**Figure 4.** Schematic sketches of sensor device (**a**) and humidity experiment set up (**b**).

recovery time was 3 min, proving a good reproducibility of the sensitivity.

A few mechanisms have been proposed for explaining the surface conductivity change in the presence of water vapour (Chou *et al* 1999; Zhao *et al* 2002; Chen and Lu 2005). In general, it experiences first the chemisorbing of monolayer water with proton transfer among hydronium ($H_3O^+$), where the electrical response depends on the number of water molecules adsorbed on the sensor surface; and

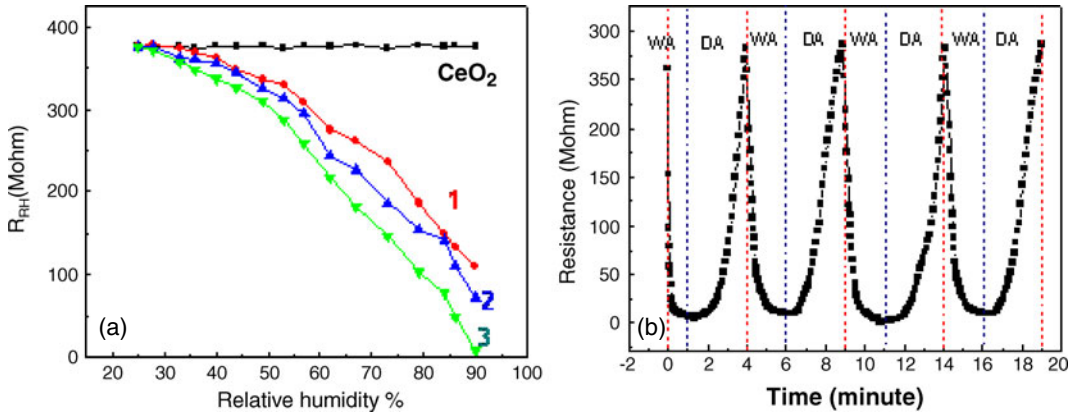


**Figure 5.** (**a**) Static response of device made of source material $CeO_2$, Mn-doped $CeO_2$ nanorods for samples 1, 2 and 3 to humidity and (**b**) dynamic response of Mn-doped $CeO_2$ of sample 3 to humidity.

then the physisorbing of multilayer water with increasing humidity, where $H_3O^+$ appears in the physisorbed water and serves as a charge carrier. $H^+$ ions can move freely in the physisorbed water according to Grotthuss's chain reaction (Anderson and Parks 1968; Sears 2000; Pokhrel and Nagaraja 2003). Electrolytic conduction takes the place of protonic conduction at high humidity. Doping Mn ions into $CeO_2$ leads to higher charge density in the surface. In this case, a strong electric field is induced around the surface of Mn-doped $CeO_2$. This strong electric field augments ionization of water molecules and further affects the deeper physisorbed water (Fu *et al* 2007). And with more Mn ions incorporation, the influence will be enhanced.

## 4. Conclusions

Mn-doped $CeO_2$ nanorods can be obtained from the reaction of $CeO_2$ particles with $MnCl_2$ through the CHM approach, which provides a one-step, convenient and low-cost route. The XPS spectra show that the manganese exists as $Mn^{4+}$. The responses to humidity for static and dynamic testing proved doping Mn into $CeO_2$ can improve the humidity sensitivity. Considering the excellent chemical and thermal stability, the Mn-doped $CeO_2$ nanorods should be a potential material for humidity detecting applications.

## Acknowledgements

This work is supported by the Youth Fund of Chongqing Jiaotong University (XN(2009)16).

## References

Anderson J H and Parks G A 1968 *J. Phys. Chem.* **72** 3362
Blanco G, Cauqui M A, Delgado J J and Galtayries A 2004 *Surf. Interface Anal*. **36** 752
Burroughs P, Hamnett A, Orchard A F and Thornton G 1976 *J. Chem. Soc. Dalton Trans*. 1686
Chen Z and Lu C 2005 *Sensor Lett*. **3** 274
Chou K S, Lee T K and Liu F J 1999 *Sensors Actuators* **B56** 106
Corma A, Atienzar P and Garc H 2004 *Nature Mater*. **3** 394
Fu Q, Deng W and Saltsburg H 2006 *Appl. Catal*. **B56** 57
Fu X Q, Wang C, Yu H C, Wang Y G and Wang T H 2007 *Nanotechnology* **18** 145503
Goi D, Leitenburg C, Dolcetti G and Trovarelli A 2004 *Environ. Technol*. **25** 1397
Hu C G, Liu H, Lao C S, Zhang L Y, Davidovic D and Wang Z L 2006 *J. Phys. Chem*. **B110** 14050
Kang CH Y, Kusaba H, Yahiro H, Sasaki K and Teraoka Y 2006 *Solid State Ionics* **177** 1799
Kim C H and Thompson L T 2006 *J. Catal*. 244
Kosynkin V D, Arzgatkina A A, Ivanov E N and Chtoutsa M G 2000 *J. Alloys Compd* **39** 1023
Leandro G R, Jose M S A and Miguel L H 2009 *Nano Lett*. **9** 1395
Machida M, Uto M, Kurogi D and Kijima T 2000 *Chem. Mater*. **12** 3158
Parvatikar N, Jain S, Bhoraskar S V and Ambika Prasad M V N 2006 *J. Appl. Polym. Sci*. **102** 5533
Pokhrel S and Nagaraja K S 2003 *Sensors Actuators* **B92** 144
Sears W M 2000 *Sensors Actuators* **B67** 161
Shan W J, Ma N, Yang J L, Dong X W, Liu C and Wei L L 2010 *J. Nat. Gas Chem*. **19** 86
Stefanik T S and Tuller H L 2001 *J. Eur. Ceram. Soc*. **21** 1967
Teraoka T, Matsumura Y, Asakura K and Kagawa S 1999 *Electrochem. Soc. Proc*. **99** 131
Wang N, Hu C G, Xia C H, Feng B, Zhang Z W and Xi Y 2007 *Appl. Phys. Lett*. **90** 163111
Wu X D, Qing L, Duan W, Jun F and Rui R 2007 *Catal. Today* **126** 430
Zhang D S, Fu H X, Shi L Y, Fang J H and Qiang L 2007 *J. Solid State Chem*. **180** 654
Zhang Z W, Hu C G, Xiong Y F, Yang R S and Wang Z L 2007 *Nanotechnology* **18** 465504
Zhao J, Bulduml A, Han J and Lu J P 2002 *Nanotechnology* **13** 195